Continuous-Time Discrete-Space Models for Animal Movement Data

Ephraim M. Hanks
Department of Statistics, Colorado State University, Fort Collins, CO,
U.S.A.
email: hanks@stat.colostate.edu

Mevin B. Hooten
U. S. Geological Survey, Colorado Cooperative Fish and Wildlife Research
Unit,
Colorado State University, Fort Collins, CO, U.S.A.

Mat W. Alldredge
Colorado Parks and Wildlife
Fort Collins, CO, U.S.A.

November 12, 2012

Abstract

The processes influencing animal movement and resource selection are complex and varied. Past efforts to model changing behavior over time used Bayesian statistical models with variable parameter space, such as reversible-jump Markov chain Monte Carlo approaches, which are computationally demanding and inaccessible to many practitioners. We present a continuous-time discrete-space (CTDS) model of animal movement that can be fit using standard generalized linear modeling (GLM) methods. This CTDS approach allows for the joint modeling of location-based as well as directional drivers of movement. Changing behavior over time is modeled using a varying-coefficient framework which maintains the computational simplicity of a GLM approach, and variable selection is accomplished using a group lasso penalty. We apply our approach to a study of two mountain lions (*Puma concolor*) in Colorado, USA.

KEYWORDS: Agent-Based Model; Animal Movement; Mountain Lion; Multiple Imputation; Varying-Coefficient Model.

1 Introduction

Animal telemetry data have been used extensively in recent years to study animal movement, space use, and resource selection (e.g., Johnson et al., 2011; Hanks et al., 2011; Fieberg et al., 2010). The ease with which telemetry data are being collected is increasing, leading to vast increases in the number of animals being monitored, as well as the temporal resolution at which telemetry locations are obtained (Cagnacci et al., 2010). This combination can result in huge amounts of telemetry data on a single animal population under study. Additionally, the processes driving animal movement are complex, varied, and changing over time. For example, animal behavior could be driven by the local environment (e.g., Hooten et al., 2010), by conspecifics or predator/prey interactions (e.g., Merrill et al., 2010), by internal states and needs (e.g., Nathan et al., 2008), or by memory (e.g., Van Moorter et al., 2009). The animal's response to each of these drivers of movement is also likely to change drastically over time (e.g., Nathan et al., 2008; Hanks et al., 2011; McClintock et al., 2012).

The large amount of telemetry data available, even for one animal, and the complex behavior displayed in animal movement results in a challenging situation for statistical modeling. There is no shortage of existing statistical models of animal movement; however, most of these models are computationally demanding, and most are inaccessible to the practitioner. For example, consider the agent-based model of animal movement of Hooten et al. (2010). The agent-based framework is highly flexible, allowing for location-based and directional drivers of movement, but is computationally expensive. Analyzing the movement path of one animal with hourly locations over the course of a week using the approach of Hooten et al. (2010) can require computational time on the order of days using standard computing resources. The velocity-based framework for modeling animal movement of Hanks et al. (2011) allows for time-varying behavior through a changepoint model of response to drivers of movement, and is more computationally efficient than the approach of Hooten et al. (2010), requiring computational time on the order of hours for a similar problem. Similarly, the mechanistic state-switching approach of McClintock et al. (2012) allows for time-varying behavior through a state-switching approach. These three approaches use Bayesian statistical models, and both Hanks et al. (2011) and McClintock et al. (2012) allow for time-varying behavior by letting the model parameter space vary, either through a reversible-jump Markov chain Monte Carlo approach (Green, 1995) or the related birth-death Markov chain Monte Carlo approach (Stephens, 2000). These methods can be quite computationally

demanding, require the user to tune the algorithm to ensure convergence, and can be inaccessible to many practitioners.

The agent-based model of Hooten et al. (2010) assumes a representation of the animal's movement path that is discrete in both space (grid cells) and time (fixed time intervals). The velocity-based movement model of Hanks et al. (2011) assumes a representation of the movement path that is continuous in space and discrete in time. The state-switching model of McClintock et al. (2012) assumes a representation of the movement path that is discrete in time and continuous in space.

In this paper, we present a continuous-time, discrete-space (CTDS) model for animal movement which allows for flexible modeling of an animal's response to drivers of movement in a computationally efficient framework. Instead of a Bayesian approach, we adopt a likelihood-based approach for inference, and instead of a state-switching or change-point model for changing behavior over time, we adopt a time-varying coefficient model. We also allow for variable selection using a lasso penalty. This CTDS approach is highly computationally efficient, requiring only minutes or seconds to analyze movement paths that would require hours using the approach of Hanks et al. (2011) or days using the approach of Hooten et al. (2010), allowing the analysis of longer movement paths and more complex behavior than has been previously possible. To make this CTDS approach for modeling animal movement and resource selection accessible to practitioners, code to implement this approach is available online (www.stat.colostate.edu/~hanks) in the form of a package for the R statistical computing environment (R Development Core Team, 2012) with worked examples.

In Section 2 *Preliminaries*, we describe the continuous-time continuous-space model of Johnson et al. (2008) which is used to make inference on the posterior predictive distribution of an animal's continuous movement path, conditioned on observed telemetry locations. We then describe the method of multiple imputation (Rubin, 1987) which we use to integrate over the uncertainty in the animal's continuous movement path. In Section 3 *Continuous-Time Discrete-Space Movement Model*, we describe the CTDS model for animal movement, and show how inference can be made on parameters in this model using standard software for generalized linear models (GLMs). In Section 4 *Time-Varying Behavior and Variable Selection* we use a varying-coefficient approach to model changing behavior over time, and use a lasso penalty for variable selection. In Section 5 *Drivers of Animal Movement* we discuss modeling potential covariates in the CTDS framework. In Section 6 *Example: Mountain Lions in Colorado* we illustrate our approach through an analysis of mountain lion (*Puma concolor*)

movement in Colorado, USA. Finally, in Section 7 *Discussion* we discuss possible extensions to the CTDS approach.

2   Preliminaries

2.1   Continuous-Time Continuous-Space Movement Model

To model animal movement, we make use of the continuous time correlated random walk (CTCRW) model of Johnson et al. (2008) to characterize a distribution for the continuous path conditioned on observed telemetry data. Let $\mathbf{S} = \{\mathbf{s}(t), t = t_0, t_1, \ldots, t_T\}$ be a collection of time-referenced telemetry locations for an animal. If the animal's location and velocity at an arbitrary time t are $\mathbf{s}(t)$ and $\mathbf{v}(t)$, respectively, then the CTCRW model can be specified as follows, ignoring the multivariate notation for simplicity:

$$v(t) = \psi_1 + \frac{\psi_2 e^{-\psi_3 t}}{\sqrt{2\psi_3}} \omega \left(e^{2\psi_3 t} \right) , \qquad (1)$$

$$s(t) = s(0) + \int_0^t v(u) du ,$$

where $\boldsymbol{\psi} = [\psi_1, \psi_2, \psi_3]$ control the movement and $\omega(t)$ is standard Brownian motion. This model can be discretized and formulated as a state-space model, which allows for efficient computation of discretized paths $\tilde{\mathbf{S}}$ at arbitrarily fine time intervals via the Kalman filter (Johnson et al., 2008). If a Bayesian framework is used for inference on $\boldsymbol{\psi}$, Johnson et al. (2008) shows how the posterior predictive distribution of the animal's continuous path $\tilde{\mathbf{S}}$ can be approximated using importance sampling. We will refer to the posterior predictive path distribution as $[\tilde{\mathbf{S}}|\mathbf{S}]$, where the bracket notation '[·]' denotes a probability distribution.

2.2   Multiple Imputation

Our general strategy is to construct a model conditioned on the continuous path $\tilde{\mathbf{S}}$, and then integrate over the uncertainty in the posterior predictive distribution $[\tilde{\mathbf{S}}|\mathbf{S}]$ (e.g., Hooten et al., 2010; Hanks et al., 2011). If we treat the unobserved continuous path $\tilde{\mathbf{S}}$ as missing data, then we can make inference on model parameters using multiple imputation (Rubin, 1987). We motivate multiple imputation as posterior predictive inference on the imputation distribution within a Bayesian framework. Our treatment is similar to that of Rubin (1987) and Rubin (1996).

If we desire posterior predictive inference $[\boldsymbol{\theta}|\mathbf{S}]$ concerning environmentally relevant movement parameters $\boldsymbol{\theta}$, conditioned on the telemetry data $\mathbf{S}$ and the posterior predictive path distribution $[\tilde{\mathbf{S}}|\mathbf{S}]$, then we can write:

$$[\boldsymbol{\theta}|\mathbf{S}] = \int_{\tilde{\mathcal{S}}} [\boldsymbol{\theta}|\tilde{\mathbf{S}}][\tilde{\mathbf{S}}|\mathbf{S}]d\tilde{\mathbf{S}}. \tag{2}$$

In the multiple imputation literature, the posterior predictive path distribution $[\tilde{\mathbf{S}}|\mathbf{S}]$ is called the imputation distribution and specifies a statistical model for the missing data $\tilde{\mathbf{S}}$ conditioned on the observed data $\mathbf{S}$. We will use the CTCRW model of Johnson et al. (2008) as the imputation distribution $[\tilde{\mathbf{S}}|\mathbf{S}]$ in our CTDS approach to modeling animal movement. The CTCRW model is a mechanistic model of animal movement that has been successfully applied to studies of aquatic (Johnson et al., 2008) and terrestrial (Hooten et al., 2010) animals, and can represent a wide range of behavior.

Hooten et al. (2010) and Hanks et al. (2011) use composition sampling to obtain samples from the posterior predictive distribution $[\boldsymbol{\theta}|\mathbf{S}]$ in (2) by sampling iteratively from $[\boldsymbol{\theta}|\tilde{\mathbf{S}}]$ and $[\tilde{\mathbf{S}}|\mathbf{S}]$. Alternately, under the multiple imputation framework the posterior distribution $[\boldsymbol{\theta}|\mathbf{S}]$ is assumed to be asymptotically Gaussian. The posterior can then be approximated using only the posterior predictive mean and variance, which can be obtained using conditional mean and variance formulae:

$$\begin{aligned}
E(\boldsymbol{\theta}|\mathbf{S}) &\approx \int_{\Theta} \boldsymbol{\theta} \int_{\tilde{\mathcal{S}}} [\boldsymbol{\theta}|\tilde{\mathbf{S}}][\tilde{\mathbf{S}}|\mathbf{S}]d\tilde{\mathbf{S}}d\boldsymbol{\theta} \\
&= \int_{\tilde{\mathcal{S}}} \left(\int_{\Theta} \boldsymbol{\theta}[\boldsymbol{\theta}|\tilde{\mathbf{S}}]d\boldsymbol{\theta} \right) [\tilde{\mathbf{S}}|\mathbf{S}]d\tilde{\mathbf{S}} \\
&= E_{\tilde{\mathbf{S}}|\mathbf{S}} \left(E(\boldsymbol{\theta}|\tilde{\mathbf{S}}) \right)
\end{aligned} \tag{3}$$

and likewise:

$$\mathrm{Var}(\boldsymbol{\theta}|\mathbf{S}) \approx E_{\tilde{\mathbf{S}}|\mathbf{S}} \left(\mathrm{Var}(\boldsymbol{\theta}|\tilde{\mathbf{S}}) \right) + \mathrm{Var}_{\tilde{\mathbf{S}}|\mathbf{S}} \left(E(\boldsymbol{\theta}|\tilde{\mathbf{S}}) \right). \tag{4}$$

As the posterior distribution $[\boldsymbol{\theta}|\tilde{\mathbf{S}}]$ converges asymptotically to the sampling distribution of the maximum likelihood estimate (MLE) of $\boldsymbol{\theta}$, we can approximate $[\boldsymbol{\theta}|\tilde{\mathbf{S}}]$ by obtaining the asymptotic sampling distribution of the MLE. This allows us to use standard maximum likelihood approaches for inference, which can be much more computationally efficient than their Bayesian counterparts for this class of models.

The multiple imputation estimate $\hat{\boldsymbol{\theta}}_{MI}$ is typically obtained by approximating the integrals in (3) and (4) using a finite sample from the imputation distribution. The procedure can be summarized as follows:

1. Draw K different realizations (imputations) $\tilde{\mathbf{S}}^{(k)} \sim [\tilde{\mathbf{S}}|\mathbf{S}]$ from the imputation distribution.

2. For each realization, find the MLE $\hat{\boldsymbol{\theta}}^{(k)}$ and asymptotic variance $Var(\hat{\boldsymbol{\theta}}^{(k)})$ of the estimate based on the the full data: $(\tilde{\mathbf{S}})$.

3. Combine results from different imputations using finite sample versions of the conditional expectation (3) and variance (4) results:

$$\hat{\boldsymbol{\theta}}_{MI} = \frac{1}{K} \sum_{k=1}^{K} \hat{\boldsymbol{\theta}}^{(k)} \tag{5}$$

$$Var(\hat{\boldsymbol{\theta}}_{MI}) = \frac{1}{K} \sum_{k=1}^{K} var(\hat{\boldsymbol{\theta}}^{(k)}) + \frac{1}{K} \sum_{k=1}^{K} \left(\hat{\boldsymbol{\theta}}^{(k)} - \bar{\hat{\boldsymbol{\theta}}} \right)^2. \tag{6}$$

Equations (5) and (6) are the commonly used combining rules (Rubin, 1987) for multiple imputation estimators in the scalar case. When $\boldsymbol{\theta}$ is vector-valued, similar approaches can be used (Rubin, 1987).

3   Continuous-Time Discrete-Space Movement Model

Having described the multiple imputation framework, we now focus on specifying a model of animal response to drivers of movement $[(\tilde{\mathbf{S}}, \mathbf{S})|\boldsymbol{\theta}]$ that is flexible and computationally efficient. In doing so, we will assume a discrete (e.g., gridded) model for space (e.g., Hooten et al., 2010), and model animal movement as a continuous-time random walk through the discrete, gridded space.

Let the the study area be defined as a graph $(\mathbf{G}, \mathbf{A})$ of M locations $\mathbf{G} = (G_1, G_2, \ldots, G_M)$ connected by "edges" $\mathbf{\Lambda} = \{\lambda_{ij} : i \sim j, i = 1, \ldots, M\}$ where $i \sim j$ means that the nodes G_i and G_j are directly connected. For example, in a gridded space each grid cell is a node and the edges connect each grid cell to its first-order neighbors (e.g., a rook's neighborhood). In typical studies, the spatial resolution of the grid cells in $\mathbf{G}$ will be determined by the resolution at which environmental covariates that may drive animal movement and selection are available.

Figure 1: Continuous-time continuous-space and continuous-time discrete-space representations of an animal's movement path.
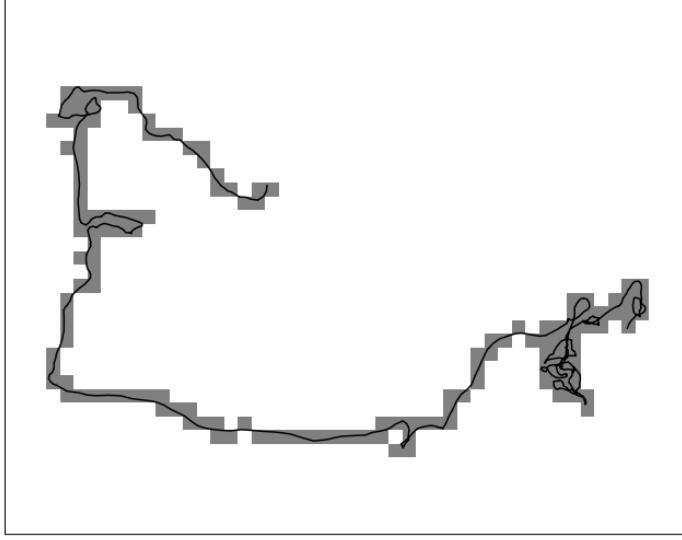
A path realization $\tilde{\mathbf{S}}$ from the CTCRW model is continuous in time and space (Figure 1). If we consider a discrete, gridded space $\mathbf{G}$, then the continuous-time, continuous-space path $\tilde{\mathbf{S}}$ is represented by a continuous-time, discrete-space path $(\mathbf{g}, \boldsymbol{\tau})$ consisting of a sequence of grid cells $\mathbf{g} = (G_{i_1}, G_{i_2}, \ldots, G_{i_T})$ transversed by the animal's continuous-space path and the residence times $\boldsymbol{\tau} = (\tau_1, \tau_2, \ldots, \tau_T)$ in each grid cell.

In practice, this transformation from continuous space to discrete space results in a compression of the data to a temporal scale that is relevant to the resolution of the environmental covariates that may be driving movement and selection. For example, if an animal is moving slow relative to the time it takes to traverse a grid cell in $\mathbf{G}$, then the quasi-continuous path $\tilde{\mathbf{S}}$ may contain a long sequence of locations within one grid cell. The discrete-space representation of the path represents this long sequence of locations as one observation (a grid cell G_{it} and residence time τ_t). This data compression

8

is especially relevant for telemetry data, in which observation windows can span years or even decades for some animals.

3.1 Random Walk Model

The discrete-space representation $(\mathbf{g}, \boldsymbol{\tau})$ of the movement path allows us to use standard discrete-space random walk models to make inference about possible drivers of movement. While we will relax this assumption later to account for temporal autocorrelation in movement behavior, we initially assume that the the t-th observation (G_{i_t}, τ_t) in the sequence is independent of all other observations in the sequence. Under this assumption, the likelihood of the sequence of transitions $\{(G_{i_t} \to G_{i_{t+1}}, \tau_t), t = 1, 2, \ldots, T\}$ is just the product of the likelihoods of each individual observation. We will focus on modeling each transition $(G_{i_t} \to G_{i_{t+1}}, \tau_t)$, and will drop the t subscript in this section to simplify notation.

If an animal is in cell G_i at time t, then define the Poisson rate of transition from cell G_i to a neighboring cell G_j as

$$\lambda_{ij}(\boldsymbol{\beta}) = \exp\{\mathbf{x}'_{ij}\boldsymbol{\beta}\} \tag{7}$$

where $\mathbf{x}_{ij}$ is a vector containing covariates related to drivers of movement specific to cells i and j, and $\boldsymbol{\beta}$ is a vector of parameters that define how each of the covariates in $\mathbf{x}_{ij}$ are correlated with animal movement. The total transition rate λ_i from cell i is the sum of the transition rates to all neighboring cells: $\lambda_i(\boldsymbol{\beta}) = \sum_{j \sim i} \lambda_{ij}(\boldsymbol{\beta})$ and the time τ that the animal resides in cell G_i is exponentially-distributed with rate parameter equal to the total transition rate $\lambda_i(\boldsymbol{\beta})$:

$$[\tau|\boldsymbol{\beta}] = \lambda_i(\boldsymbol{\beta}) \exp\left\{-\tau \lambda_i(\boldsymbol{\beta})\right\}. \tag{8}$$

When the animal transitions from cell G_i to one of its neighbors, the probability of transitioning to cell G_k, an event we denote as $G_i \to G_k$, follows a multinomial distribution with probability proportional to the transition rate λ_{ik} to cell G_k:

$$[G_i \to G_k|\boldsymbol{\beta}] = \frac{\lambda_{ik}(\boldsymbol{\beta})}{\sum_{j \sim i} \lambda_{ij}(\boldsymbol{\beta})} = \frac{\lambda_{ik}(\boldsymbol{\beta})}{\lambda_i(\boldsymbol{\beta})}. \tag{9}$$

If, as is commonly assumed in the study of Markov random walks, the residence time and eventual destination are independent events, then the likelihood of the observation $(G_i \to G_k, \tau)$ is the product of the likelihoods of its parts:

$$[G_i \to G_k, \tau | \boldsymbol{\beta}] = \frac{\lambda_{ik}(\boldsymbol{\beta})}{\lambda_i(\boldsymbol{\beta})} \cdot \lambda_i(\boldsymbol{\beta}) \exp\left\{-\tau \lambda_i(\boldsymbol{\beta})\right\}$$
$$= \lambda_{ik}(\boldsymbol{\beta}) \exp\left\{-\tau \lambda_i(\boldsymbol{\beta})\right\}. \tag{10}$$

3.2 Latent Variable Representation

We now introduce a latent variable representation of the transition process that is equivalent to (10), but allows for inference within a standard generalized linear modeling framework. For each j such that $i \sim j$, define z_j as

$$z_j = \begin{cases} 1 & , \; G_i \to G_j \\ 0 & , \; \text{o.w.} \end{cases}$$

and let

$$[z_j, \tau | \boldsymbol{\beta}] \propto \lambda_{ij}^{z_j} \exp\left\{-\tau \lambda_{ij}(\boldsymbol{\beta})\right\} \tag{11}$$

where n_i is the number of neighbors of the i-th grid cell. Then the product of $[z_j, \tau | \boldsymbol{\beta}]$ over all j such that $i \sim j$ is proportional to the likelihood (10) of the observed transition:

$$\prod_{j:i\sim j} [z_j, \tau | \boldsymbol{\beta}] \propto \prod_{j:i\sim j} \lambda_{ij}^{z_j} \exp\left\{-\tau \lambda_{ij}(\boldsymbol{\beta})\right\}$$
$$= \lambda_{ik}(\boldsymbol{\beta}) \exp\left\{-\tau \lambda_i(\boldsymbol{\beta})\right\} \; , \; \text{where } G_i \to G_k$$
$$= [G_i \to G_k, \tau | \boldsymbol{\beta}]$$

The benefit of this latent variable representation is that the likelihood of $z_j, \tau | \boldsymbol{\beta}$ in (11) is equivalent to the kernel of the likelihood in a Poisson regression with the canonical log link, where z_j are the observations and $\log(\tau)$ is an offset or exposure term. The likelihood of the entire continuous-time, discrete-space path $(\mathbf{g}, \boldsymbol{\tau})$ can be written (returning t to the notation) as:

$$[\mathbf{g}, \boldsymbol{\tau} | \boldsymbol{\beta}] = [\mathbf{Z}, \boldsymbol{\tau} | \boldsymbol{\beta}] \propto \prod_{t=1}^{T} \prod_{i_t \sim j_t} \left[\lambda_{i_t j_t}^{z_{j_t}}(\boldsymbol{\beta}) \exp\{-\tau_t \lambda_{i_t j_t}(\boldsymbol{\beta})\} \right] \tag{12}$$

where $\mathbf{Z} = (\mathbf{z}_1, \ldots, \mathbf{z}_T)'$ is a vector containing the latent variables $\mathbf{z}_i = (z_{i_1}, z_{i_2}, \ldots, z_{i_K})'$ for each grid cell in the discrete-space path. Inference can be made on $\boldsymbol{\beta}$ in (12) using standard Poisson GLM approaches (e.g., maximum likelihood). This provides a computationally efficient framework for the statistical analysis of potential drivers of movement within the multiple

10

imputation framework of Section 2.2. Multiple path realizations (imputations) can be drawn from $[\tilde{\mathbf{S}}|\mathbf{S}]$. Each continuous path $\tilde{\mathbf{S}}$ can then be transformed into a CTDS path $(\mathbf{g}, \boldsymbol{\tau})$, which can then be used to make inference on $\boldsymbol{\beta}$ using (12). The results from the multiple imputed paths can then be combined using (5) and (6), resulting in a multiple imputation estimate $\hat{\boldsymbol{\beta}}_{MI}$ and estimated variance $Var(\hat{\boldsymbol{\beta}}_{MI})$.

4 Time-Varying Behavior and Variable Selection

In this section we describe how covariate effects can be allowed to vary over time using a varying-coefficient model, and how variable selection can be accomplished through shrinkage estimation.

4.1 Changing Behavior Over Time

Animal behavior and response to drivers of movement can change significantly over time. These changes can be driven by external factors such as changing seasons (e.g., Grovenburg et al., 2009) or predator/prey interactions (e.g., Lima, 2002), or by internal factors such as internal energy levels (e.g., Nathan et al., 2008). The most common approach to modeling time-varying behavior in animal movement is state-space modeling, typically within a Bayesian framework (e.g., Morales et al., 2004; Jonsen et al., 2005; Getz and Saltz, 2008; Nathan et al., 2008; Forester et al., 2009; Gurarie et al., 2009; Merrill et al., 2010). Often, the animal is assumed to exhibit a number of behavioral states, each characterized by a distinct pattern of movement or response to drivers of movement. The number of states can be either known and specified in advance by the researcher (e.g., Morales et al., 2004; Jonsen et al., 2005) or allowed to be random (e.g., Hanks et al., 2011; McClintock et al., 2012).

State-space models are an intuitive approach to modeling changing behavior over time, but there are limits to the complexity that can be modeled using this approach. Allowing the number of states to be unknown and random requires a Bayesian approach with a changing parameter space. This is typically implemented using reversible-jump MCMC methods (e.g., Green, 1995; McClintock et al., 2012; Hanks et al., 2011), which are computationally expensive and can be difficult to tune. Our approach is to use a computationally efficient GLM (12) to analyze parameters related to drivers of animal movement. Instead of using the common state-space approach, we employ varying-coefficient models (e.g., Hastie and Tibshirani, 1993) to model time-varying behavior in animal movement.

For simplicity in notation, consider the case where there is only one covariate x in the model (7) and no intercept term. The model for the Poisson transition rate (7) will typically contain an intercept term and multiple covariates $\{x\}$, and the varying-coefficient approach we present generalizes easily to this case. In a time-varying-coefficient model, we allow the parameter $\beta(t)$ to vary over time in a functional (continuous) fashion. The transition rate (7) then becomes:

$$\lambda_{ij}(\beta(t)) = \exp\{x_{ij}\beta(t)\}$$

where t is the time of the observation and x_{ij} is the value of the covariate related to the Poisson rate of moving from cell i to cell j. The functional regressor $\beta(t)$ is typically modeled as a linear combination of n_{spl} spline basis functions $\{\phi_k(t), k = 1, \ldots, n_{spl}\}$:

$$\beta(t) = \sum_{k=1}^{n_{spl}} \alpha_k \phi_k(t).$$

B-spline basis functions are among the most-widely used choices for $\{\phi_k(t)\}$, and are appropriate in most cases. Fourier basis functions are commonly used for $\{\phi_k(t)\}$ when the behavior is thought to be periodic (e.g., diurnal variation in behavior).

Under this varying-coefficient specification, (7) can be rewritten as

$$
\begin{aligned}
\lambda_{ij}(\beta(t)) &= \exp\{x_{ij}\beta(t)\} \\
&= \exp\left\{x_{ij}\sum_{k=1}^{n_{spl}} \alpha_k \phi_k((t))\right\} \\
&= \exp\left\{\phi'_{ij}\alpha\right\}
\end{aligned}
\tag{13}
$$

where $\alpha = (\alpha_1, \ldots, \alpha_{n_{spl}})'$ and $\phi_{ij} = x_{ij} \cdot (\phi_1(t), \ldots, \phi_{n_{spl}}(t))'$. The result is that the varying-coefficient model can be written as a GLM with a modified design matrix. This specification provides a flexible framework for allowing the effect of a driver of movement (x) to vary over time that is computationally efficient and simple to implement using standard GLM software.

4.2 Shrinkage Estimation

The model we have specified in (12) is likely to be overparameterized, especially if we utilize a varying-coefficient model (13). Animal movement

behavior is complex, and a typical study could entail a large number of potential drivers of movement, but an animal's response to each of those drivers of movement is likely to change over time, with only a few drivers being relevant at any one time. Under these assumptions, many of the parameters α_k in (13) are likely to be very small or zero. Multicollinearity is also a potential problem, as many potential drivers of movement could be correlated with each other.

We propose a shrinkage estimator of $\boldsymbol{\alpha}$ using a lasso penalty (Tibshirani, 1996). The typical maximum likelihood estimate of $\boldsymbol{\alpha}$ is obtained by maximizing the likelihood $[\mathbf{Z}, \boldsymbol{\tau} | \boldsymbol{\alpha}]$ from (12), or equivalently by maximizing the log-likelihood $\log[\mathbf{Z}, \boldsymbol{\tau} | \boldsymbol{\alpha}]$. The lasso estimate is obtained by maximizing the penalized log-likelihood, where the penalty is the sum of the absolute values of the regression parameters $\{\alpha_k\}$:

$$\hat{\boldsymbol{\alpha}}_{\text{lasso}} = \max_{\boldsymbol{\alpha}} \left\{ \log[\mathbf{Z}, \boldsymbol{\tau} | \boldsymbol{\alpha}] - \gamma \sum_{k=1}^{K} |\alpha_k| \right\}. \tag{14}$$

As the tuning parameter γ increases, the absolute values of the regression parameters $\{\alpha_k\}$ are "shrunk" to zero, with the parameters that best describe the variation in the data being shrunk more slowly than parameters that do not. Cross-validation is typically used to set the tuning parameter γ at a level that optimizes the model's predictive power.

Shrinkage approaches such as the lasso are well-developed for GLMs, and computationally-efficient methods are available for fitting GLMs to data (e.g., Friedman et al., 2010). Recent work has also applied the lasso to multiple imputation estimators (e.g., Chen and Wang, 2011). The main challenge in applying the lasso to multiple imputation is that a parameter may be shrunk to zero in the analysis of one imputation but not in the analysis of another. The solution is to use a so-called group lasso (Yuan and Lin, 2006), in which a group of parameters is constrained to either all equal zero or all be non-zero together.

The lasso can be seen as a constrained optimization problem, with $\boldsymbol{\alpha}_{\text{lasso}}$ minimizing the mean squared error subject to the constraint that $||\boldsymbol{\alpha}_{\text{lasso}}||_1 \leq \nu$, where $|| \cdot ||$ is the L-1 norm and the value of ν is determined by the tuning parameter γ. As the estimate $\boldsymbol{\alpha}_{\text{lasso}}$ typically falls on the boundary of the constrained space, conventional approaches for estimating the standard error of $\boldsymbol{\alpha}_{\text{lasso}}$ are unavailable. Bayesian versions of the lasso (Park and Casella, 2008) and group lasso (Raman et al., 2009) provide alternatives that allow for estimation of the uncertainty about the parameters $\boldsymbol{\alpha}_{\text{lasso}}$ through posterior analysis.

The Bayesian approach entails significantly more computational complexity, and may not be as accessible to practitioners. We instead focus on the likelihood-based stacked lasso estimate of Chen and Wang (2011). In this estimate, instead of computing the lasso estimate $\boldsymbol{\alpha}_{\text{lasso}}$ for each imputation individually, and then combining the results using (5) and (6), the imputed data from all estimates are "stacked" together and a group lasso estimate is obtained for the combined data. We note that this likelihood-based stacked lasso approach does not allow for the estimation of the variance of $\boldsymbol{\alpha}_{\text{lasso}}$. If uncertainty estimates are a priority, we recommend choosing a parsimonious selection of potential drivers of movement *a priori* that exhibit little multicollinearity and computing the traditional multiple imputation estimates $\hat{\boldsymbol{\alpha}}_{MI}$.

5 Drivers of Animal Movement

We now provide some examples showing how a range of hypothesized drivers of movement could be modeled within the CTDS framework. Following Hooten et al. (2010), we consider two distinct categories for drivers of movement from cell G_i to cell G_j: location-based drivers ($\{p_{ki}, k = 1, 2, \ldots, K\}$) which are determined only by the characteristics of cell G_i, and directional drivers ($\{q_{lij}, l = 1, 2, \ldots, L\}$) which vary with direction of movement. Under a time-varying coefficient model for each driver, the transition rate (7) from cell G_i to cell G_j is

$$\lambda_{ij}\left(\beta(t)\right) = \exp\left\{\beta_0(t) + \sum_{k=1}^{K} p_{ki}\beta_k(t) + \sum_{l=1}^{L} q_{lij}\beta_l(t)\right\} \tag{15}$$

where $\beta_0(t)$ is a time-varying intercept term, $\{\beta_k(t)\}$ are time-varying effects related to location-based drivers of movement, and $\{\beta_l(t)\}$ are time-varying effects related to directional drivers of movement. We consider both location-based and directional drivers in what follows.

5.1 Location-Based Drivers of Movement

Hooten et al. (2010) denote static, non-directional drivers of movement as location-based drivers of movement. Location-Based drivers of movement can be used to examine differences in animal movement rates that can be explained by the environment an animal resides in. In the CTDS context, location-based drivers would be covariates dependent only on the characteristics of the cell where the animal is currently located. Large positive

(negative) values of the corresponding $\beta_k(t)$ would indicate that the animal tends to transition quickly (slowly) from a cell containing the cover type in question.

5.2   Directional Drivers of Movement

In contrast to location-based drivers, which describe the effect that the local environment in which the animal resides has on movement rates, directional drivers of movement (Brillinger et al., 2001; Hooten et al., 2010; Hanks et al., 2011) capture directional selection by the individual.

A directional driver of movement is defined by a vector which points toward (or away) from something that is hypothesized to attract (or repel) the animal in question. Let $\mathbf{v}_l$ be the vector corresponding to the l-th directional driver of movement. In the CTDS model for animal movement, the animal can only transition from cell G_i to one of its neighbors $G_j : j \sim i$. Let $\mathbf{w}_{ij}$ be a unit vector pointing from the center of cell G_i in the direction of the center of cell G_j. Then the covariate q_{lij} relating the l-th directional driver of movement to the transition rate from cell G_i to cell G_j is the dot (or inner) product of $\mathbf{v}_l$ and $\mathbf{w}_{ij}$:

$$q_{lij} = \mathbf{v}_l'\mathbf{w}_{ij}.$$

Then p_{lij} will be positive when $\mathbf{v}_l$ points nearly in the direction of cell G_j, negative when $\mathbf{v}_l$ points directly away from cell G_j, and zero if $\mathbf{v}_l$ is perpendicular to the direction from cell G_i to cell G_j.

5.3   Examples

We now provide multiple examples of drivers of movement to illustrate the range of effects that can be modeled using this framework.

5.3.1   Overall Movement Rate

The intercept term $\beta_0(t)$ in (15) can be seen as a driver of movement in which $p_{0i} = 1$ for every cell $G_i \in \mathbf{G}$. This intercept term controls the animal's overall rate of transition from any cell, and thus models the animal's overall movement rate. Allowing the intercept parameter $\beta_0(t)$ to vary over time could reveal changes in activity levels over time. For example, we might expect $\beta_0(t)$ to be larger at night for nocturnal species and smaller during the day.

15

5.3.2 Movement Response to Land Cover Types

Indicator variables could be used to examine how animal movement differs between different landscape cover types (e.g., forest vs. plains) by setting $p_{ki} = 1$ for each cell G_i that is classified as containing the k-th cover type. As in the case of the intercept, allowing the parameter $\beta_k(t)$ related to the k-th cover type to vary over time can reveal variation in an animal's movement pattern through the cover type. For example, an animal may move quickly through open terrain during the day, but may move more slowly through the same terrain at night.

5.3.3 Environmental Gradients

Animals may use environmental gradients for navigation. For example, a mule deer might move predominantly in the direction of increasing elevation during a spring migration (e.g., Hooten et al., 2010), or a seal might follow gradients in sea surface temperature to navigate toward land (e.g., Hanks et al., 2011). Such effects can be modeled by including a directional driver of movement in (15) defined by a gradient vector $\mathbf{v}_l$ which points from the center of cell G_i in the direction of steepest increase in the covariate x_l. Positive values of β_l indicate that the animal moves generally towards cells with higher values of x_l, while negative values of β_l indicate that the animal moves generally towards cells with lower values of x_l.

5.3.4 Activity Centers

Many animals exhibit movement patterns that are centered on a location in space. This central location may be temporary, such as a kill site for a predator (e.g., Knopff et al., 2009), or more permanent, such as a den for a central place forager (e.g., Hanks et al., 2011; McClintock et al., 2012). The relatively new class of spatial capture-recapture models (e.g., Royle and Young, 2008) model detection probability as a decreasing function of distance from a central location (e.g., the "center" of an animal's home range). Movement around an activity center can be modeled in the CTDS framework by including a directional driver of movement in (15) defined by a vector $\mathbf{v}_l$ which points from the center of cell G_i to the location of the activity center. Then a positive value for β_l would indicate that the animal is generally drawn toward this activity center. If the activity center is considered to be temporary (such as a kill site for a predator), then a time-varying-coefficient model should be used. The variable selection obtained through the lasso estimate can indicate the range of time in which the animal's movement is

centered around the activity center. If the activity center is considered to be permanent through the duration of the study, a varying-coefficient model may not be needed.

Under the likelihood-based specification of the CTDS model for animal movement, it is necessary to specify the locations of all hypothesized activity centers beforehand. In Section 6, we show an example of the specification of hypothesized activity centers (potential kill sites for mountain lions) using the original telemetry data. If a Bayesian formulation of the CTDS model were used, then the location of hypothesized activity centers could be random, and inference could be made on their locations jointly with inference on the movement parameters, similar to what is done in spatial capture-recapture models (e.g., Royle and Young, 2008).

5.3.5   Conspecific Interaction

An animal's movement patterns can be greatly affected by interaction with conspecifics. For example, one animal could follow the trail left by another animal, two animals could avoid one another by changing course when they become close enough to sense the other animal, or a pair of animals could maintain proximity as they move together across the landscape. While there are many possible approaches to modeling such dependence in behavior, we choose to model each of these interactions through the inclusion of directional effects in the CTDS modeling framework. For example, a directional driver could be included in the movement model for one animal that is defined by a vector pointing to the current location of another animal to examine whether the animal being modeled is attracted to ($\beta_l > 0$) or avoids ($\beta_l < 0$) the conspecific.

5.3.6   Directional Persistence

The CTCRW model of Johnson et al. (2008) is based on a correlated random walk model for velocity that allows for directional persistence in animal movement. So far, we have assumed that each discrete movement step in our CTDS model is independent, but this assumption is not met if the animal exhibits any directional persistence. To account for directional persistence in the CTDS approach, we use an autoregressive approach by including a directional driver of movement at each discrete movement step that is defined by a vector pointing in the direction of the previous move. For example, if the animal moved west in the previous discrete movement step, then the autoregressive vector for the next step points west as well. Positive values

of the β related to this directional driver of movement indicate that the animal is likely to maintain its direction of movement over time.

5.4   Spatial and Temporal Scale

The choice of scale for a study can greatly influence results (e.g., Boyce, 2006). When speaking of the scale of a study, one could look at the grain, or resolution, at which the process is modeled, or the extent (coverage) over which the process is modeled. The spatial and temporal extent of a study of animal movement are determined by the telemetry data and the posterior predictive path distribution $[\tilde{\mathbf{S}}|\mathbf{S}]$. However, when implementing the CTDS approach, the researcher must make three choices pertaining to the grain or resolution: (1) the temporal scale at which the CTCRW movement path of the animal is sampled, (2) the spatial scale of the grid over which the discrete-space movement will be modeled, and (3) the temporal scale of the varying coefficient model, which is determined by the number and resolution of spline knots in the spline basis expansion.

As the CTCRW model of Johnson et al. (2008) is a continuous-time model, we recommend sampling from the movement path at as fine an interval as is feasible. In practice, this will be limited by computational resources and the size of the study. The temporal resolution needs to be fine enough that realizations from the posterior predictive path distribution $[\tilde{\mathbf{S}}|\mathbf{S}]$ are quasi-continuous and adequately capture the residence time τ in each grid cell in the CTDS representation of the movement path.

The choice of spatial resolution of the raster grid on which the CTDS process occurs implicitly specifies a time scale at which the movement process is modeled. Coarser spatial resolution (larger grid cells) will correspond to longer residence times τ in the CTDS mode. The spatial resolution should be chosen so that the time scale at which an animal transitions from one grid cell to another is a time scale at which the animal in question can make meaningful choices about movement and resource selection. The time scale implicit in the choice of spatial resolution can be examined by plotting a histogram of the residence times in the CTDS representation of the movement path.

If the lasso penalty is used, then it is common to choose a saturated spline basis expansion in the varying-coefficient model, where one spline knot is specified at each data point in time. We recommend specifying a spline basis expansion with knots at a similar temporal resolution to the temporal resolution of the telemetry data. The lasso penalization will shrink the overparameterized expansion to a more parsimonious model that best

fits the data. While a finer temporal resolution could be used, the posterior predictive path distribution is unlikely to show changes in behavior at time scales smaller than the time scale of the original data. Using a coarser temporal resolution will force $\beta(t)$ to be smooth. This would imply that changes in animal behavior are gradual and occur at time scales larger than the time scale of the data.

6 Example: Mountain Lions in Colorado

We illustrate our CTDS random walk approach to modeling animal movement through a study of mountain lions (*Puma concolor*) in Colorado, USA. As part of a larger study, a female mountain lion, designated AF79, and her subadult cub, designated AM80, were fitted with global positioning system (GPS) collars set to transmit location data every 3 hours. We analyze the location data **S** from one week of location information for these two animals (Figure 2).

We fit the CTCRW model of Johnson et al. (2008) to both animals' location data using the 'crawl' package (Johnson, 2011) in the R statistical computing environment (R Development Core Team, 2012). Ten imputations from the posterior distribution of the quasi-continuous path distribution $[\tilde{\mathbf{S}}|\mathbf{S}]$ were obtained at one-minute intervals. The result is a quasi-continuous path at extremely fine temporal resolution for each imputation.

For covariate data, we used a landcover map of the state of Colorado created by the Colorado Vegetation Classification Project (http://ndis.nrel.colostate.edu/coveg/), which is a joint project of the Bureau of Land Management and the Colorado Division of Wildlife. The landcover map contained gridded landcover information at 100m square resolution. Figure 3 shows a histogram of the residence times $\boldsymbol{\tau}$ in each grid cell in the CTDS representation of the movement path of AM80. The area traveled by the two animals in our study was predominantly forested. To assess how the animals' movement differed when in terrain other than forest, we created an indicator covariate where all forested grid cells were assigned a value of zero, and all cells containing other cover types, including developed land, bare ground, grassland, and shrubby terrain, were assigned a value of one (Figure 2a). This covariate and an intercept covariate were used as location-based covariates in the CTDS model for both animals.

For each animal, we created a set of potential kill sites (PKS) by examining the original GPS location data (Figure 2). Knopff et al. (2009) classified a location as a PKS if two or more GPS locations were found within 200m

Figure 2: Telemetry data for a female mountain lion (AF79) and her male cub (AM80). A location-based covariate was defined by landcover that was not predominanty forested (a). Potential kill sites were identified, and a directional covariate defined by a vector pointing toward the closest kill site (b) was also used in the CTDS model.
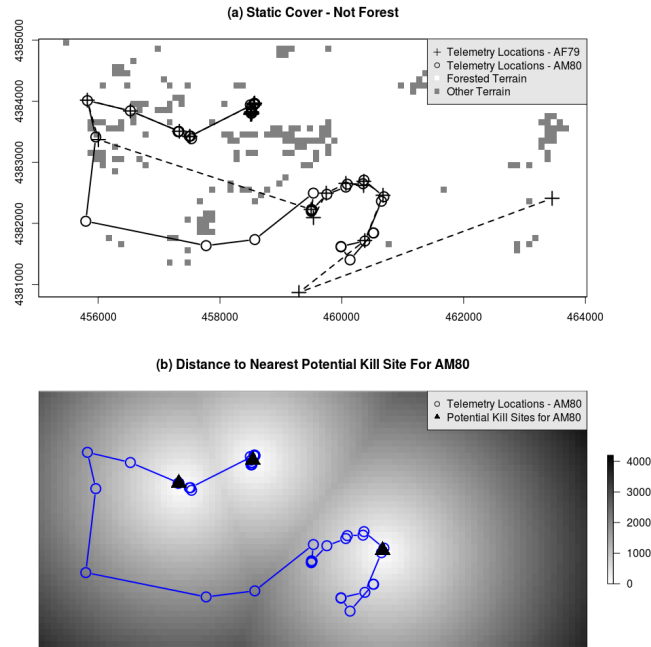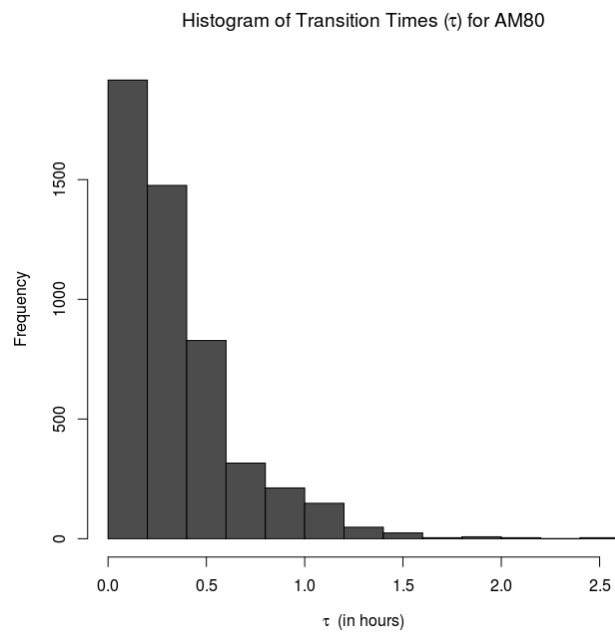
Figure 3: Histogram of residence times in each 100m-square grid cell in the continuous-time discrete-space representation of the movement path of a male mountain lion (AM80).

Histogram of Transition Times (τ) for AM80

of the site within a six-day period. We added an additional restraint that at least one of the GPS locations be during nighttime hours (9pm to 6am) for the point to be classified a PKS. We then created a covariate raster layer containing the distance to the nearest PKS for each grid cell (Figure 2). A directional covariate defined by a vector pointing towards the nearest PKS was included in the CTDS model for both animals.

To examine how the movement path of the cub AM80 affected the movement path of the mother AF79, we included a directional covariate in the CTDS model for AF79 defined by a vector pointing from the mother's location to the cub's location at each time point. Similarly, we included a directional covariate in the CTDS model for AM80 defined by a vector pointing from the cub's location to the mother's location at each time point.

For each animal, we also included a directional covariate pointing in the direction of the most recent movement at each time point. This covariate measures the strength of correlation between moves, and thus the strength of the directional persistence shown by the animal's discrete-space movement path. As we are assuming an underlying correlated movement model (the CTCRW model of Johnson et al. (2008)), we expect the CTDS movement to be correlated in time as well.

To allow for varying behavior over time, we used a varying-coefficient model for each covariate in the model. For all covariates except the directional covariate related to directional persistence, we used a B-spline basis expansion, with regularly spaced spline knots at 3-hour intervals.

We fit the CTDS model for each path using the 'glmnet' R package (Friedman et al., 2010), using a Lasso penalty, with tuning parameter chosen to minimize the average squared error of the fit in a 10-fold cross-validation.

6.1 Results

The time-varying results for the location-based and directional drivers of movement for AF79 are shown in Figure 4, with the corresponding results for AM80 shown in Figure 5. As we used a lasso penalty, we can only obtain point estimates (confidence intervals are unavailable) of the time-varying effects $\{\beta(t)\}$. A comparison of the differences between the results for AF79 and AM80 yields some insight into how the movement patterns of these two animals differ.

The intercept effect measures the animal's general movement rate over time. Figure 4(a) and Figure 5(a) show the time-varying deviation from the grand mean for each animal. For example, the male AM80 moved at a higher than average rate of speed near sunrise on Julian day 90, as evidenced by the

Figure 4: Time-varying results for the location-based and directional covariates in the continuous-time discrete-space model for a female mountain lion (AF79). Shaded regions indicate nighttime hours.
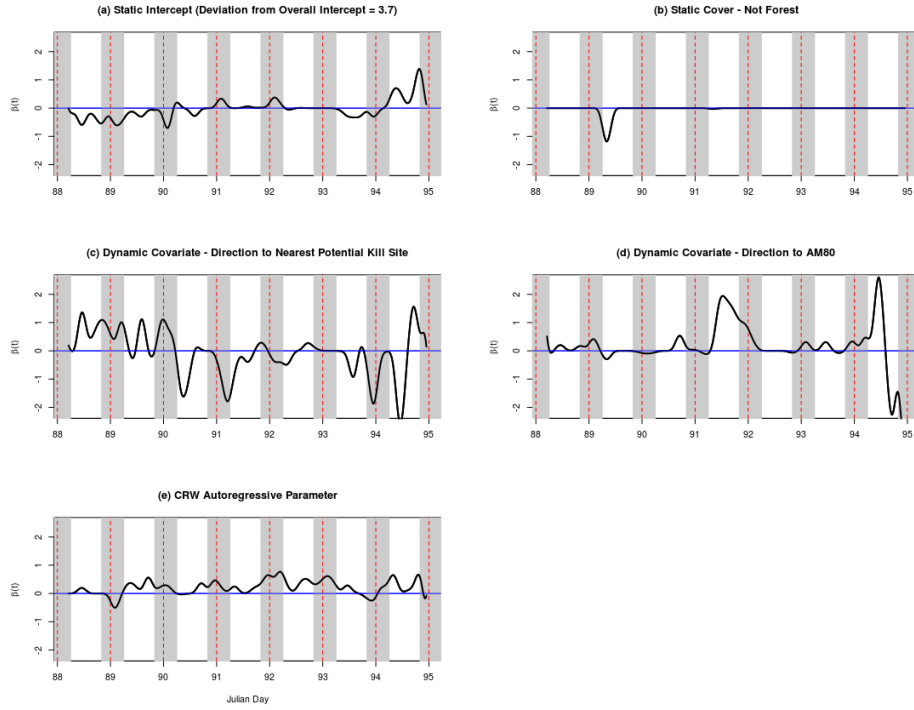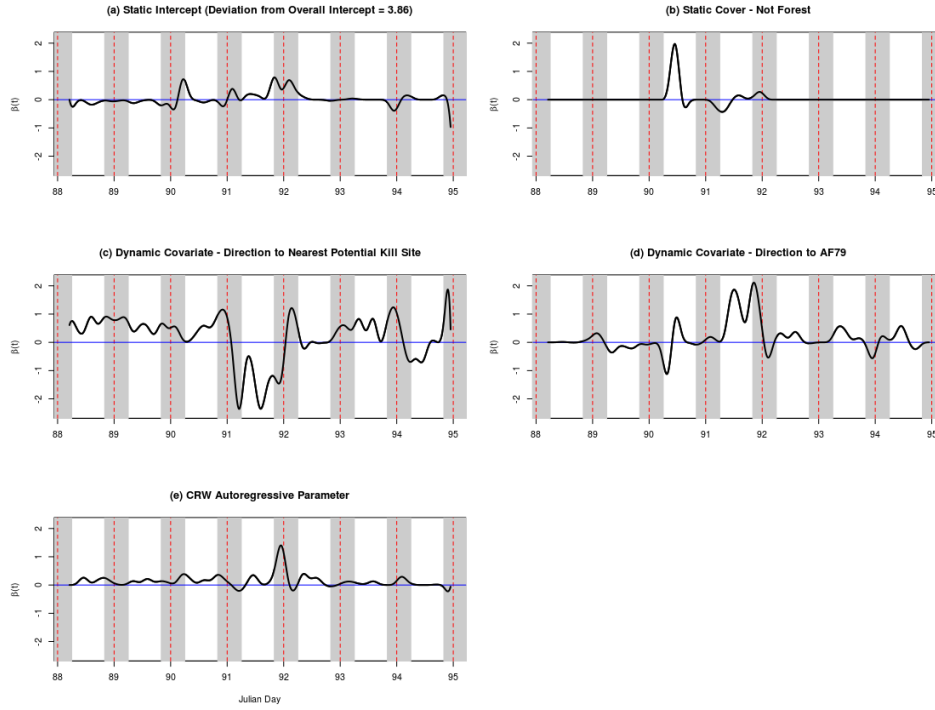
Figure 5: Time-varying results for the location-based and directional covariates in the continuous-time discrete-space model for a male mountain lion (AM80). Shaded regions indicate nighttime hours.

24

positive $\beta(t)$ in Figure 5(a). The time-varying intercept for both lions tends to be higher during nighttime hours and crepuscular periods than during the day, indicating higher overall rates of movement during nocturnal hours.

The location-based response to non-forested land cover (Figure 4b and Figure 5b) is zero for much of the study window for both AF79 and AM80. Forested land cover makes up over 90% of the study area, thus the mountain lions encounter different land cover infrequently. On day 90, the male (AM80) moves through a patch of non-forested land cover at a relatively high rate of speed. On day 89, the female moves through a patch of non-forested land cover at a low rate of speed. Both animals encounter non-forested patches at other times during the observation window, but the $\beta(t)$ related to movement through non-forested terrain is near-zero during these times. This $\beta(t)$ has been shrunk to zero by the Lasso procedure during these times, indicating that during these times the animal's movement is not greatly different in non-forested patches than it is in forested patches.

The male cub (AM80) has a fairly consistent positive response to the directional covariate pointing toward the nearest PKS from day 88 to day 90 (Figure 5c), indicating that much of the male's movement during these three days resembles a random walk centered on an attractive central location (a PKS). During day 91, the negative response to the direction to the nearest PKS indicates that the animal is moving away from the nearest PKS. At the same time, the positive response to the directional covariate pointing towards AF79 (Figure 5d) indicates that AM80 is moving towards AF79 during this time period.

Positive values of the autoregressive parameter (Figure 4e and Figure 5e) indicate that the animals are in a state of correlated movement (directional persistence). The magnitude of the autoregressive parameter is greater in general for the female (Figure 4e) than for the male (Figure 5e), indicating that the female may have a greater tendency for directed movements than the male. The CTDS movement paths are based on the CTCRW model of animal movement, which results in correlated movement paths. The inclusion of this autoregressive parameter is meant to account for the correlation in the CTDS path representation of the underlying correlated CTCRW movement path.

7 Discussion

While we have couched our CTDS approach in terms of modeling animal movement, we can also view this approach in terms of resource selection

(e.g., Manly, 2002). Johnson et al. (2008) describe a general framework for the analysis of resource selection from telemetry data using a weighted distribution approach where an observed distribution of resource use is seen as a re-weighted version of a distribution of available resources, and the resource selection function (RSF) defines the preferential use of resources by the animal. Warton and Shepherd (2010) and Aarts et al. (2012) describe a point-process approach to resource selection that can be fit using a Poisson GLM, similar to the CTDS model we describe here. In the context of Warton and Shepherd (2010), the CTDS approach can be viewed as a resource-selection analysis with the available resources at any time defined as the neighboring grid cells. The transition rate (15) of the CTDS process to each neighboring cell contains information about the availability of each cell, as well as the RSF that defines preferential use of the resources in each cell.

It is notable that the entire analysis in Section 6 requires less than ten minutes using a computer with 4 GB of memory and a 1.67 GHz quad-core processor. This increase in computational efficiency relative to the approaches of Johnson et al. (2008), Hooten et al. (2010), Hanks et al. (2011), and McClintock et al. (2012) allows for inference on complex behavior at finer temporal resolution than has been possible previously. To make our CTDS approach accessible to practitioners, we have created an R-package ('ctds') that contains R-code to fit the CTDS model using multiple imputation as described in Sections 2-4. A script file contained in the 'ctds' package allows for the re-analysis of the telemetry data of the two mountain lions analyzed in Section 6. This R-package can be downloaded from the first author's website (http://www.stat.colostate.edu/~hanks).

The CTDS approach to modeling animal movement is flexible, and can be extended using standard approaches for GLMs. For example, if population-level inference is desired, the movement paths from multiple animals could be analyzed jointly, with population-level parameters in the GLM being shared by all animals. Similarly, interaction terms could be included in the model by including multiplied covariates in the design matrix. Fitting movement models in a GLM framework allows for many natural extensions with little additional effort.

We have focused on building an individual model for animal movement that is intuitive and computationally-efficient. If population-level inference on data from multiple animals is desired, there are multiple potential approaches. The first is to analyze movement paths from multiple animals jointly, with population-level parameters in the GLM being shared by all animals and individual variation modeled using standard random effects approaches. However, this approach may not be straightforward to implement

or interpret in the context of a varying-coefficient model. Each individual animal is likely to encounter and be influenced by different drivers of movement (e.g., local environmental factors or nearby conspecifics) at differing times throughout the observation window. In this situation, it may make little sense to examine a population-level response to a particular driver of movement at a particular time, as in a typical random-effects analysis.

Instead, one approach to a population-level analysis could be a post-hoc analysis of the time-varying response to covariates $\boldsymbol{\beta}(t)$. For example, Hanks et al. (2011) used a cluster analysis to examine different movement regimes shared across individuals in the population. Differences in the movement patterns exhibited by subgroups (e.g., male vs. female) were then examined by a comparison of the proportion of time spent by each subgroup in each of the movement regimes.

The use of directional drivers of movement has a long history. Brillinger et al. (2001) model animal movement as a continuous-time, continuous-space random walk where the drift term is the gradient of a "potential function" that defines an animal's external drivers of movement. Tracey et al. (2005) use circular distributions to model how an animal moves in response to a vector pointing towards an object that may attract or repel the animal. Hanks et al. (2011) and McClintock et al. (2012) make extensive use of gradients to model directed movements, and movements about a central location. In our study of mountain lion movement data, we used directional drivers of movement to model conspecific interaction between a mother (AF79) and her cub (AM80). Interactions between predators and prey could also be modeled using directional covariates defined by vectors pointing between animals. Some movements based on memory could also be modeled using directional covariates. For example, a directional covariate defined by a vector pointing to the animal's location one year prior could be used to model seasonal migratory behavior. The ability to model both location-based and directional drivers of movement make the CTDS framework a flexible and extensible framework for modeling complex behavior in animal movement.

References

Aarts, G., Fieberg, J., and Matthiopoulos, J. (2012). Comparative interpretation of count, presence–absence and point methods for species distribution models. *Methods in Ecology and Evolution* **3,** 177–187.

Boyce, M. (2006). Scale for resource selection functions. *Diversity and Distributions* **12,** 269–276.

Brillinger, D., Preisler, H., Ager, A., and Kie, J. (2001). *The use of potential functions in modeling animal movement*, chapter 24. Nova Publishers.

Cagnacci, F., Boitani, L., Powell, R. a., and Boyce, M. S. (2010). Animal ecology meets GPS-based radiotelemetry: a perfect storm of opportunities and challenges. *Philosophical Transactions of the Royal Society of London. Series B, Biological Sciences* **365,** 2157–62.

Chen, Q. and Wang, S. (2011). Variable selection for multiply-imputed data with application to dioxin exposure study. Technical Report 217, University of Wisconsin-Madison Department of Biostatistics and Medical Informatics.

Fieberg, J., Matthiopoulos, J., Hebblewhite, M., Boyce, M. S., and Frair, J. L. (2010). Correlation and studies of habitat selection: problem, red herring or opportunity? *Philosophical transactions of the Royal Society of London. Series B, Biological sciences* **365,** 2233–44.

Forester, J. D., Im, H. K., and Rathouz, P. J. (2009). Accounting for animal movement in estimation of resource selection functions: sampling and data analysis. *Ecology* **90,** 3554–65.

Friedman, J., Hastie, T., and Tibshirani, R. (2010). Regularization paths for generalized linear models via coordinate descent. *Journal of statistical software* **33,** 1.

Getz, W. and Saltz, D. (2008). A framework for generating and analyzing movement paths on ecological landscapes. *Proceedings of the National Academy of Sciences* **105,** 19066.

Green, P. J. (1995). Reversible jump markov chain monte carlo computation and bayesian model determination. *Biometrika* **82,** 711.

Grovenburg, T., Jenks, J., Klaver, R., Swanson, C., Jacques, C., and Todey, D. (2009). Seasonal movements and home ranges of white-tailed deer in north-central south dakota. *Canadian Journal of Zoology* **87,** 876–885.

Gurarie, E., Andrews, R. D., and Laidre, K. L. (2009). A novel method for identifying behavioural changes in animal movement data. *Ecology Letters* **12,** 395–408.

Hanks, E., Hooten, M., Johnson, D., and Sterling, J. (2011). Velocity-based movement modeling for individual and population level inference. *PLoS ONE* **6,** e22795.

Hastie, T. and Tibshirani, R. (1993). Varying-Coefficient Models. *Journal of the Royal Statistical Society: Series B (Statistical Methodology)* **55,** 757–796.

Hooten, M. B., Johnson, D. S., Hanks, E. M., and Lowry, J. H. (2010). Agent-based inference for animal movement and selection. *Journal of Agricultural, Biological, and Environmental Statistics* **15,** 523–538.

Johnson, D., London, J., and Kuhn, C. (2011). Bayesian Inference for Animal Space Use and Other Movement Metrics. *Journal of Agricultural, Biological, and Environmental Statistics* **16,** 357–370.

Johnson, D., London, J., Lea, M., and Durban, J. (2008). Continuous-time correlated random walk model for animal telemetry data. *Ecology* **89,** 1208–1215.

Johnson, D., Thomas, D., Ver Hoef, J., and Christ, A. (2008). A general framework for the analysis of animal resource selection from telemetry data. *Biometrics* **64,** 968–976.

Johnson, D. S. (2011). *crawl: Fit continuous-time correlated random walk models for animal movement data.* R package version 1.3-2.

Johnson, D. S., Thomas, D. L., Ver Hoef, J. M., and Christ, A. (2008). A general framework for the analysis of animal resource selection from telemetry data. *Biometrics* **64,** 968–76.

Jonsen, I., Flemming, J., and Myers, R. (2005). Robust state-space modeling of animal movement data. *Ecology* **86,** 2874–2880.

Knopff, K., Knopff, A., Warren, M., and Boyce, M. (2009). Evaluating global positioning system telemetry techniques for estimating cougar predation parameters. *The Journal of wildlife management* **73,** 586–597.

Lima, S. (2002). Putting predators back into behavioral predator–prey interactions. *Trends in Ecology & Evolution* **17,** 70–75.

Manly, B. (2002). *Resource selection by animals: statistical design and analysis for field studies.* Springer.

McClintock, B. T., King, R., Thomas, L., Matthiopoulos, J., McConnell, B., and Morales, J. (2012). A general discrete-time modeling framework for animal movement using multi-state random walks. *Ecological Monographs* page In Press.

Merrill, E., Sand, H., Zimmermann, B., McPhee, H., Webb, N., Hebble-white, M., Wabakken, P., and Frair, J. L. (2010). Building a mechanistic understanding of predation with GPS-based movement data. *Philosophical Transactions of the Royal Society B: Biological Sciences* **365,** 2279–2288.

Morales, J. M., Haydon, D. T., Frair, J., Holsinger, K. E., and Fryxell, J. M. (2004). Extracting more out of relocation data: building movement models as mixtures of random walks. *Ecology* **85,** 2436–2445.

Nathan, R., Getz, W., Revilla, E., Holyoak, M., Kadmon, R., Saltz, D., and Smouse, P. (2008). A movement ecology paradigm for unifying organismal movement research. *Proceedings of the National Academy of Sciences* **105,** 19052.

Park, T. and Casella, G. (2008). The Bayesian lasso. *Journal of the American Statistical Association* **103,** 681–686.

R Development Core Team (2012). *R: A Language and Environment for Statistical Computing.* R Foundation for Statistical Computing, Vienna, Austria.

Raman, S., Fuchs, T., Wild, P., Dahl, E., and Roth, V. (2009). The bayesian group-lasso for analyzing contingency tables. In *Proceedings of the 26th Annual International Conference on Machine Learning*, pages 881–888. ACM.

Royle, J. and Young, K. (2008). A hierarchical model for spatial capture-recapture data. *Ecology* **89,** 2281–2289.

Rubin, D. B. (1987). *Multiple Imputation for Nonresponse in Surveys.* John Wiley and Sons, New York, New York, USA.

Rubin, D. B. (1996). Multiple imputation after 18+ years. *Journal of the American Statistical Association* **91,** 473.

Stephens, M. (2000). Bayesian analysis of mixture models with an unknown number of components - an alternative to reversible jump methods. *The Annals of Statistics* **28,** 40–74.

Tibshirani, R. (1996). Regression shrinkage and selection via the lasso. *Journal of the Royal Statistical Society. Series B (Methodological)* pages 267–288.

Tracey, J. a., Zhu, J., and Crooks, K. (2005). A set of nonlinear regression models for animal movement in response to a single landscape feature. *Journal of Agricultural, Biological, and Environmental Statistics* **10,** 1–18.

Van Moorter, B., Visscher, D., Benhamou, S., Börger, L., Boyce, M. S., and Gaillard, J.-M. (2009). Memory keeps you at home: a mechanistic model for home range emergence. *Oikos* **118,** 641–652.

Warton, D. and Shepherd, L. (2010). Poisson point process models solve the pseudo-absence problem for presence-only data in ecology. *The Annals of Applied Statistics* **4,** 1383–1402.

Yuan, M. and Lin, Y. (2006). Model selection and estimation in regression with grouped variables. *Journal of the Royal Statistical Society: Series B (Statistical Methodology)* **68,** 49–67.